Solid State Communications 252 (2017) 64–67

Contents lists available at ScienceDirect

Solid State Communications

journal homepage: www.elsevier.com/locate/ssc

Communication

Raman spectroscopy of the superconductor $CuCrO_2$ delafossite oxide

J.F.H.L. Monteiro[a], A.R. Jurelo[a], E.C. Siqueira[b,*]

[a] Departamento de Física, Universidade Estadual de Ponta Grossa - UEPG, 84030-000 Ponta Grossa, PR, Brasil
[b] Departamento de Física, Universidade Tecnológica Federal do Paraná - UTFPR, 84016-210 Ponta Grossa, PR, Brasil

A B S T R A C T

Polycrystalline $CuCrO_2$ samples were successfully prepared by traditional solid-state reaction method and using self-combustion urea nitrate process. The crystal structure and the effect of the sample preparation on the Raman vibrational modes were systematically investigated. Raman spectra at room temperature were obtained with light focused on several points inside a single grain. Phonon modes allowed by symmetry were identified, besides of some additional lines. Significant differences in phonon modes between samples prepared by solid state reaction method and self-combustion urea nitrate process were observed.

1. Introduction

Materials with a delafossite-type structure has attracted great interest due to their thermoelectric, optoelectric, electric, magnetic and recently also superconductor properties [1,2]. The delafossite belongs to a family of ternary oxides with formula ABO_2. This crystal consists of stacking of BO_2 layers made of edge-sharing BO_6 octahedra that are connected by planes of A cations arranged as a triangular pattern with respect to the *c*-axis [3]. The monovalent cations A (Cu, Ag, Pd or Pt) are linearly coordinated by two oxygen ions, while the trivalent cations B are located in distorted edge-shared BO_6 octahedra [3]. The cation B may be replaced by: a *p*-block metal (Ga, In and Al), a transition metal (Fe, Cr, Co and Y) or a rare earth element (La, Nd and Eu) [3].

Depending on the composition, these oxides can exhibit conductivities ranging from insulating to semimetallic. Most widely studied transparent *p*-type oxides are in the Cu-based delafossite crystal. In particular, $CuCrO_2$ has received great attention. Its conductivity is about 1 scm^{-1} (thin film) but, upon doping with 5% Mg, can be improved to 220 scm^{-1}, the highest *p*-type conductivity [4]. Also, $CuCrO_2$ has good optical transparency in the visible range with a band gap of about 3.1 eV [5]. These materials exhibit also unique magnetic and electric properties. $CuCrO_2$ is multiferroic (exhibits simultaneously ferromagnetic and ferroelectric orders), with antiferromagnetic and ferroelectric orders below its Néel temperature (25 K) [6], and ferromagnetism in room- and low-temperature [7].

Recently, Katayama-Yoshida et al. studied superconductivity in hole-doped delafossite $CuAlO_2$ [1]. Shifting the Fermi level using FLAPW method, they proposed that the nesting Fermi surface may cause a strong-phonon interaction. By using density functional perturbation theory, the electron-phonon interaction and the critical temperature (T_C) of *p*-doped $CuAlO_2$ were calculated [2]. They obtained a T_C around 50 K, suggesting that hole-doped $CuAlO_2$ may be a superconductor. Taddee et al. investigated the effects of Fe concentration on the microstructural, optical, magnetic and electrical properties of $CuCr_{1-x}Fe_xO_2$ delafossite oxide [2]. The polycrystalline samples were synthesized using a self-combustion urea nitrate process. By magnetic hysteresis loop measurements, it was showed that the Fe-doped $CuCrO_2$ exhibited ferromagnetic behavior at room temperature, while resistivity measurements revealed superconductivity below 118 and 89 K, for x=0.00 and 0.10 samples, respectively [2]. Different methods of preparation of $CuCrO_2$ samples have been reported in literature, such as reactive sputtering deposition [8], pulsed laser deposition [9] and solid state reaction [10]. However, to our knowledge, only by self-combustion urea nitrate process the superconductivity was observed [2].

To study the doping effect on the delafossite structure, Raman spectroscopy may be used. For Al-doped samples, Amami et al. concluded that the Al substitution does not change the structure of this material, but produces a strengthening of (Cr, Al)-O bond [11]. Pellicer-Porres et al. investigated the vibrational modes of $CuGaO_2$ delafossite prepared by ceramic method by means of Raman experiments at ambient and high pressures [12]. Two Raman-active modes were observed, and experiments indicated the existence of a phase transition at 26 GPa, and that was related with the existence of a dynamical instability at about the same pressure [12]. Yet, the same authors studied the vibrational properties of single crystals of $CuAlO_2$ by means of Raman scattering in ambient conditions, low temperature

* Corresponding author.
E-mail address: ecosta@utfpr.edu.br (E.C. Siqueira).

http://dx.doi.org/10.1016/j.ssc.2017.01.014
Received 24 December 2016; Accepted 15 January 2017
Available online 17 January 2017

and high pressure [13]. The single crystals were grown from a $CuAl_2O_4$-CuO melt by a slow cooling method [13,14]. A reversible phase transition at 34 GPa was also observed and related to the existence of a dynamical instability [13].

In this work, we study the vibrational modes of $CuCrO_2$ delafossite oxide. The polycrystalline samples for this study were successfully prepared by traditional solid-state reaction method (not superconductor) and using self-combustion urea nitrate process (superconductor). The crystal structure and the effect of the sample preparation on the Raman vibrational modes were systematically investigated.

2. Experimental details

In order to compare the vibrational modes of $CuCrO_2$ delafossite oxide, three set of polycrystalline samples were prepared: one set prepared by traditional solid-state reaction method and two sets prepared by self-combustion urea nitrate process. For the sample prepared by conventional solid-state reaction (labeled sample I), stoichiometric amounts of CuO and Cr_2O_3 were mixed and calcinated at 1000 °C for 10 h. Then, the calcined mixtures were ground again, pressed into pellets, and sintered at 1000 °C for more 10 h.

For self-combustion urea nitrate process, the samples (labeled samples II and III) were prepared by using $Cu(NO_3)_2{\cdot}3H_2O$), $Cr(NO_3)_3{\cdot}0.9H_2O$ and urea as precursor materials (high purities). As in Ref. [2], the desired quantities of precursor materials were dissolved in deionized water to form a mixed solution. Then, urea nitrate were used and after continuous stirring at around 360 K by 1 h, the precursor solution was heated at approximately 470 K. After, the obtained material was heated in a crucible on a hot plate at 570 K. The product was calcined at 1050 K for 3 h in a N_2 atmosphere, and then the powder was ground again and pressed into pellets and finally sintered in air at 1250 K by 3 h. For this process, the sample obtained was called sample III.

The sample calcined at 1050 K for 3 h in air (not in N_2 atmosphere) was labeled as sample II.

The crystallinity and microstructure of the samples were checked by scanning electron microscopy (SEM) and X-ray diffraction (XRD). In order to study the vibrational modes, unpolarized confocal Raman measurements were performed with a Bruker Senterra R200-532 spectrometer equipped with an Olympus optical microscope and with a thermo-electrically cooled CCD detector. Acquisition times ranged around 20 s with an incident laser power density below 60×10^{-4} W/cm^2.

3. Results and discussion

The phase of $CuCrO_2$ samples was characterized by powder XRD. Fig. 1 shows the XRD patterns taken at room temperature for $CuCrO_2$ samples prepared by different methods: (a) solid-state reaction method, (b) self-combustion urea nitrate without N_2 and (c) self-combustion urea nitrate with N_2 process. Almost all reflections can be assigned to the delafossite structure with space group $R\bar{3}m$. For identifying possible structural distortion or impurity phase, we performed Rietveld refining of the data, as well as the use of the standard JCPDS card of $CuCrO_2$ and CuO. It was observed a very small difference between the two samples prepared by self-combustion urea nitrate, but a great difference between them and the sample prepared by solid state reaction. Yet, the relative strength of the peaks is the same from the JCPDS standard for the sample prepared by self-combustion urea nitrate with and without N_2. Also, for samples prepared by self-combustion urea nitrate, small quantities of the secondary phase of CuO [identified by * in Figs. 1(b) and (c)] were also observed.

The lattice parameters a, b, c and the unit cell volume V for $CuCrO_2$ samples obtained through Rietveld refinements at room temperature are summarized in Table 1. The numbers in parentheses indicate the standard deviation. The values of the lattice parameter are different for samples prepared by solid state reaction and self combustion, but are approximately the same for the samples prepared by self combustion (without and with N_2). The value of the parameter a=b is 2.9811 Å for samples prepared by the solid state method and 2.97458/2.97478 Å for self combustion, approximately 0.2% higher. On the other hand, the parameter c did not changed (only 0.01%). Consequently, the unit cell volume decreased from 131.63 Å (solid state) to 131.039/131.062 Å (self combustion), approximately 0.4–0.5% lower. Yet, in a general manner, the lattice parameters derived are in agreement with published results obtained in other studies [2,11]. Also, as the R_i factors [χ^2, $R(F^2)$ and R_{wp}] are small, the results presented are reliable. These factors are also listed in Table 1.

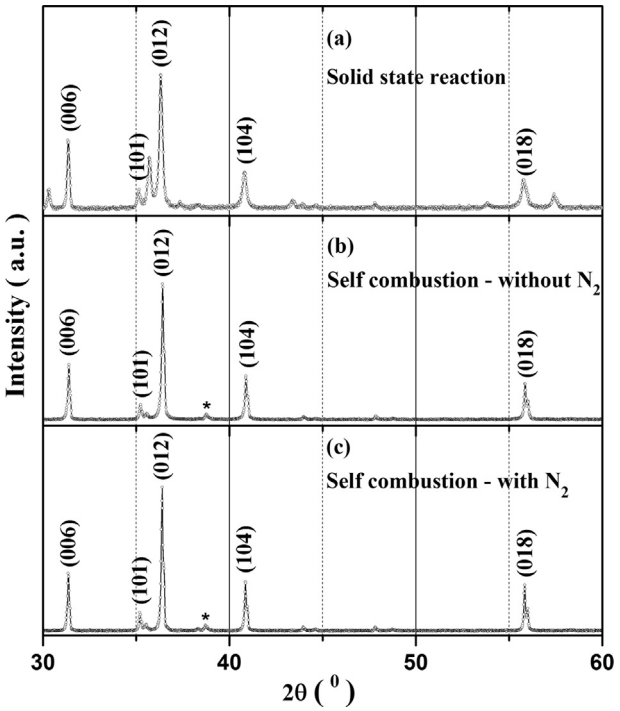

Fig. 1. (Color online) XRD patterns taken at room temperature for $CuCrO_2$ samples prepared by different methods. Secondary phase of CuO was observed (*).

Table 1
Lattice parameters a, b and c (in Å) and unit cell volume V (in Å^3) for $CuCrO_2$ samples. Numbers in parentheses indicate the standard deviation. The corresponding R_i factors are also presented.

	Solid State Reaction	*Self Combustion (without N_2)*	*Self Combustion (with N_2)*
a=b	2.9811(1)	2.97458(2)	2.97478(2)
c	17.1032(8)	17.1008(2)	17.1015(1)
V	131.63(1)	131.039(2)	101.062(1)
R_i factors			
χ^2	1.7	1.3	2.4
$R(F^2)(\%)$	20%	3%	4%
$R_{wp}(\%)$	15%	8.5%	7.3%

The crystal structure of the delafossite may be either hexagonal, described by the $P6_3/mmc$ space group symmetry, or rhombohedral, described by the $R\bar{3}m$ space group. It depends on the orientation of each layer in stacking. Also, as it has four atoms in the primitive cell, 12 optical phonon modes (=$A_{1g} + E_g + 3A_{2u} + 3E_u$) are possible in the zone center: three acoustic and nine optical modes. But, only two Raman modes are active with $A_{1\,g}$ and E_g symmetries. In the A mode, we have movement in the direction of Cu-O bonds, that is, along the hexagonal c axis, while the double degenerate E modes describe vibrations in the perpendicular direction (along the a-axis).

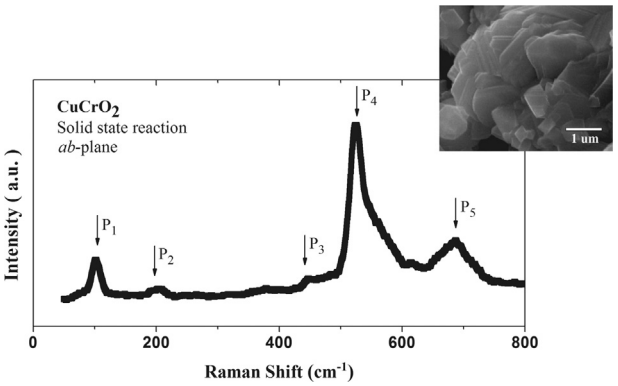

Fig. 2. (Color online) Raman spectrum for $CuCrO_2$ sample in the *ab*-plane obtained by applying a power of 20 mW at 300 K. Sample I was prepared by a conventional solid-state reaction. Upper inset: Backscattered electrons SEM micrographs in higher magnification revealing the lamellar polycrystalline microstructure.

To study the effect of the preparation sample on the structure and consequently on the superconductivity, Raman spectroscopy was performed with a solid state laser with λ=532 nm excitation light. The Raman spectra were obtained at room temperature with applied power of 20 mW (60×10^{-4} W cm^2). This power showed the best signal-to-noise ratio with well-resolved Raman peaks. The measurements were done with light focused on several points inside a single grain on the $a(b)c$-plane of $CuCrO_2$, fundamental to ensure spectra representability. In the upper inset of Fig. 2, we can observe backscattered electrons SEM micrographs for a lamellar polycrystalline sample of $CuCrO_2$ in higher magnification. The polycrystalline $CuCrO_2$ sample consists of lamellar grains with diameter in the range 2–5 μm.

The Raman spectra are shown in Figs. 2, 3 and 4. For all samples, five Raman modes were observed at the lower frequency range (0–800 cm^{-1}). These data are summarized in Table 2 with the corresponding peaks labeled from P_1 to P_5. When comparing the samples prepared by solid state reaction and by self-combustion method, one observes a noticeable shift of the peaks. However, the peaks for samples II and III exhibit just a slight fluctuation in their relative locations.

The results in this work are consistent with previous reports in

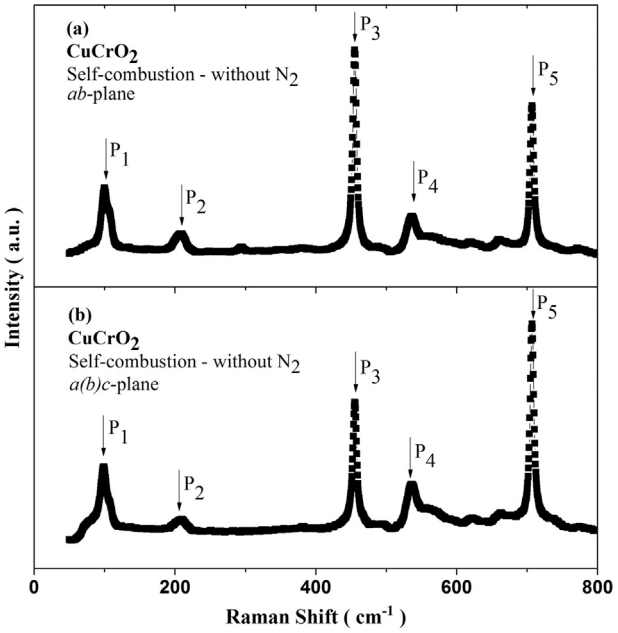

Fig. 3. (Color online) Raman spectra for $CuCrO_2$ sample in the (a) *ab*-and (b) $a(b)c$-plane obtained by applying a power of 20 mW at 300 K. The sample was synthesized using a self-combustion urea nitrate process without calcination in a N_2 atmosphere.

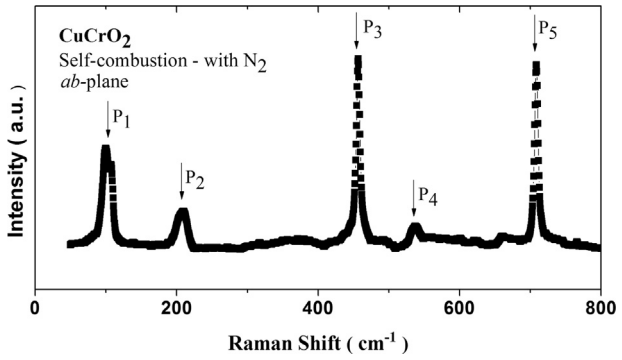

Fig. 4. (Color online) Raman spectra for $CuCrO_2$ sample in the *ab*-plane obtained by applying a power of 20 mW at 300 K. The sample was synthesized using a self-combustion urea nitrate process with calcination in a N_2 atmosphere.

Table 2
Raman-scattering data in $CuCrO_2$ samples.

Peaks	Frequency (cm^{-1}) *ab*-plane	Frequency (cm^{-1}) *a*(*b*)*c*-plane
Solid State Reaction		
P_1	102 ± 1	
P_2	204 ± 2	
P_3	449 ± 1	
P_4	525 ± 3	
P_5	688 ± 1	
Self-Combustion (*without* N_2)		
P_1	100 ± 1	99 ± 1
P_2	209 ± 2	210 ± 1
P_3	456 ± 1	456 ± 1
P_4	537 ± 1	537 ± 2
P_5	707 ± 2	707 ± 2
Self-Combustion (*with* N_2)		
P_1	100 ± 1	
P_2	210 ± 1	
P_3	457 ± 2	
P_4	538 ± 1	
P_5	708 ± 1	

literature [11–18]. In fact, from Raman spectra of $CuCr_{1-x}Al_xO_2$, three peaks were observed [11] around 207 cm^{-1}, 444 cm^{-1} and 691 cm^{-1}. For peaks localized in 207 and 691 cm^{-1}, A_{1g} modes were associated, while that for the 444 cm^{-1} peak, the E_g mode was identified. Also, Pellicer-Porres et al. studied [13] the pressure and temperature dependence of the lattice dynamics of $CuAlO_2$ single crystals by Raman scattering. Results obtained from framework of an *ab-initio* calculation, yield 770 and 433 cm^{-1} for the A_{1g} and E_g modes, respectively. A result of 767.2 cm^{-1} was observed when the polarizations of the incident and backscattered beams are parallel, but not visible with crossed polarization. From these results they concluded that this is the A_{1g} mode. Based on these earlier studies, we ascribe P_2 and P_5 peaks to A_{1g} modes while P_3 corresponds to E_g mode. The additional peaks P_1 and P_4 can also be identified with previous reports. In fact, the Raman spectrum for $CuCrO_2$ was studied in Ref. [15] with modes observed at 104, 207, 382, 457, 538, 623, 668, and 709 cm^{-1} with the peaks 457 cm^{-1} and 709 cm^{-1} being ascribed to E_g and A_{1g} modes, respectively.

By considering the *ab*-plane, it is evident by comparing Figs. 2 and 3(a) that there are significant differences between the two spectra. Indeed, the peak P_4 is the highest one for sample I but appears strongly suppressed for sample II. Additionally, the peak P_3 appears to be the highest one for sample II but is found suppressed in the spectrum for sample I. The intensity of peak P_5 has a significant increase for sample II as one can observe by a direct comparison of Figs. 2 and 3. The pattern for sample II remains qualitatively the same for $a(b)c$-plane as

shown in Fig. 3(b). Minor differences may also be noted for P_1 and P_2 which are reinforced for sample II. This is more evident for sample III, prepared by self-combustion and under N_2 atmosphere. Actually, the increase of peak P_1 is accompanied by a slight split as evident from Fig. 4.

The results presented show that the preparation method has a direct influence on the Raman spectra. This might have an important effect on the superconductivity since its possible origin has been ascribed to the strong electron-phonon interaction [1,2]. By comparing the Raman spectrum of sample I (not superconductor) with that of samples II and III (superconductors), one might relate the strong electron phonon interaction to the increase of P_3 and P_5 modes. These modes correspond to E_g and $A_{1\,g}$ symmetries, respectively, and may be a signature of electron-phonon interactions on the superconductivity of $CuCrO_2$.

It is worth noting that for $CuAlO_2$, the phonon modes ranging from 700–900 cm^{-1} give a large contribution for electron-phonon interaction [1]. However, it lacks a similar theoretical analysis for $CuCrO_2$ which would allow to determine which modes are in fact contributing to the superconducting properties of $CuCrO_2$.

4. Conclusions

Polycrystalline samples of the $CuCrO_2$ superconductor were prepared using solid state reaction method and self-combustion urea nitrate process. Raman scattering experiments were performed at room temperature with light focused on several points inside a single grain on ab- and $a(b)c$-planes. All phonon modes allowed by symmetry were found and identified. Moreover, some additional Raman modes were also observed, that can be associated with inhomogeneous microstructure.

The qualitative differences between the Raman spectra, for the sample prepared by solid state reaction in comparison to the samples prepared by self-combustion, constitute a signature of the phonon modes changes due to the preparation process. These changes may be related to the superconductivity of $CuCrO_2$ as reported in Ref. [2]. Additional studies addressing the calculation of the electron-phonon interaction in terms of the changes reported in this work may be useful in order to understand the superconductivity in this material.

Acknowledgements

This work was partially financed by CNPq under contract nº 472.746/2013-8.

References

[1] A. Nakanishi, H. Katayama-Yoshida, Computational materials design for superconductivity in hole-doped delafossite $CuAlO_2$ transparent superconductors, Solid State Commun. 152 (2012) 24–27.
[2] C. Taddee, T. Kamwanna, V. Amornkitbamrung, Characterization of transparent superconductivity fe-doped $CuCrO_2$ delafossite oxide, Applied Surface Science 380 (2016) 237–242. Proceedings for International Conference on Surfaces, Coatings and Nanostructured Materials (NANOSMAT-10, Manchester, UK).
[3] M.A. Marquardt, N.A. Ashmore, D.P. Cann, Crystal chemistry and electrical properties of the delafossite structure, Thin Solid Films 496 (2006) 146–156. in: Proceedings of the Fourth International Symposium on Transparent Oxide Thin Films for Electronics and Optics (TOEO-4).
[4] J. Tate, M. Jayaraj, A. Draeseke, T. Ulbrich, A. Sleight, K. Vanaja, R. Nagarajan, J. Wager, R. Hoffman, p-type oxides for use in transparent diodes, Thin Solid Films 411 (2002) 119–124. in: Proceedings of the 2nd International Symposium on Transparent Oxide Thin Films for Electronics and Optics.
[5] R. Nagarajan, N. Duan, M. Jayaraj, J. Li, K. Vanaja, A. Yokochi, A. Draeseke, J. Tate, A. Sleight, p-type conductivity in the delafossite structure, International Journal of Inorganic Materials 3 (2001) 265–270. University of California Santa Barbara Conference papers.
[6] K. Kimura, H. Nakamura, K. Ohgushi, T. Kimura, Magnetoelectric control of spin-chiral ferroelectric domains in a triangular lattice antiferromagnet, Phys. Rev. B 78 (2008) 140401.
[7] Y.F. Wang, Y.J. Gu, T. Wang, W.Z. Shi, Magnetic, optical and electrical properties of mn-doped $CuCrO_2$ thin films prepared by chemical solution deposition method, J. Sol.-Gel Sci. Technol. 59 (2011) 222.
[8] R.-S. Yu, C.-M. Wu, Characteristics of p-type transparent conductive $CuCrO_2$ thin films, Appl. Surf. Sci. 282 (2013) 92–97.
[9] K. Tonooka, N. Kikuchi, Preparation of transparent $CuCrO_2$:Mg/Zno junctions by pulsed laser deposition, Thin Solid Films 515 (2006) 2415–2418.
[10] T. Okuda, N. Jufuku, S. Hidaka, N. Terada, Magnetic, transport, and thermoelectric properties of the delafossite oxides CuCr(1-x)MgxO_2, Phys. Rev. B 72 (2005) 144403.
[11] M. Amami, C. Colin, P. Strobel, A.B. Salah, Al-doping effect on the structural and physical properties of delafossite-type oxide $CuCrO_2$, Physica B: Condens. Matter 406 (2011) 2182–2185.
[12] J. Pellicer-Porres, A. Segura, C. Ferrer-Roca, D. Martínez-García, J.A. Sans, E. Martínez, J.P. Itié, A. Polian, F. Baudelet, A. Mu noz, P. Rodríguez-Hernández, P. Munsch, Structural evolution of the $CuGaO_2$ delafossite under high pressure, Phys. Rev. B 69 (2004) 024109.
[13] J. Pellicer-Porres, D. Martínez-García, A. Segura, P. Rodríguez-Hernández, A. Mu noz, J.C. Chervin, N. Garro, D. Kim, Pressure and temperature dependence of the lattice dynamics of $CuAlo_2$ investigated by raman scattering experiments and ab initio calculations, Phys. Rev. B 74 (2006) 184301.
[14] M.S. Lee, T.Y. Kim, D. Kim, Anisotropic electrical conductivity of delafossite-type $CuAlO_2$ laminar crystal, Appl. Phys. Lett. 79 (2001).
[15] O. Aktas, K.D. Truong, T. Otani, G. Balakrishnan, M.J. Clouter, T. Kimura, G. Quirion, Raman scattering study of delafossite magnetoelectric multiferroic compounds: $CuFeO_2$ and $CuCrO_2$, J. Phys.: Condens. Matter 24 (2012) 036003.
[16] J. Shu, X. Zhu, T. Yi, Retracted $CuCrO_2$ as anode material for lithium ion batteries, Electrochim. Acta 54 (2009) 2795–2799.
[17] M. Amami, F. Jlaiel, P. Strobel, A.B. Salah, structural and magnetic studies of the cucr1-xrhxo2 delafossite solid solution with 0 < x < 0.2, Mater. Res. Bull. 46 (2011) 1729–1733.
[18] S. Zheng, G. Jiang, J. Su, C. Zhu, The structural and electrical property of $CuCr_{1-x}Ni_xO_2$ delafossite compounds, Mater. Lett. 60 (2006) 3871–3873.